Ligand Binding to Heme Proteins: III. FTIR Studies of His-E7 and Val-E11 Mutants of Carbonmonoxymyoglobin

David P. Braunstein, Kelvin Chu, Karen D. Egeberg, Hans Frauenfelder, Judith R. Mourant, G. Ulrich Nienhaus, Pal Ormos, Stephen G. Sligar, Barry A. Springer, and Robert D. Young
Departments of Biochemistry, Chemistry, and Physics, University of Illinois at Urbana-Champaign, Urbana, Illinois, USA

ABSTRACT Fourier-transform infrared (FTIR) difference spectra of several His-E7 and Val-E11 mutants of sperm whale carbonmonoxymyoglobin were obtained by photodissociation at cryogenic temperatures. The IR absorption of the CO ligand shows characteristic features for each of the mutants, both in the ligand-bound (*A*) state and in the photodissociated (*B*) state. For most of the mutants, a single *A* substate band is observed, which points to the crucial role of the His-E7 residue in determining the *A* substate spectrum of the bound CO in the native structure. The fact that some of the mutants show more than one stretch band of the bound CO indicates that the appearance of multiple *A* substates is not exclusively connected to the presence of His-E7. In all but one mutant, multiple stretch bands of the CO in the photodissociated state are observed; these *B* substates are thought to arise from discrete positions and/or orientations of the photodissociated ligand in the heme pocket. The red shifts of the *B* bands with respect to the free-gas frequency indicate weak binding in the heme pocket. The observation of similar red shifts in microperoxidase (MP-8), where there is no residue on the distal side, suggests that the photodissociated ligand is still associated with the heme iron. Photoselection experiments were performed to determine the orientation of the bound ligand with respect to the heme normal by photolyzing small fractions of the sample with linearly polarized light at 540 nm. The resulting linear dichroism in the CO stretch spectrum yielded angles $\alpha \geq 20°$ between the CO molecular axis and the heme normal for all of the mutants. We conclude that the off-axis position of the CO ligand in the native structure does not arise from steric constraints imposed by the distal histidine. There is no clear correlation between the size of the distal residue and the angle α of the CO ligand.

INTRODUCTION[1]

Hemoglobin and myoglobin utilize the heme prosthetic group, Fe-protoporphyrin IX, to perform their oxygen transport and storage function. Free heme in solution would not function as a physiological oxygen carrier because of its fast autoxidation rate and because it binds CO 10^3–10^4 times more tightly than O_2 (Collman et al., 1976). The production of CO in the endogenous breakdown of heme would make reversible oxygenation impossible. To accomplish reversible oxygen binding, the protein provides significant discrimination between CO and O_2 in favor of dioxygen (Stryer, 1988), and it also prevents autoxidation of the heme iron. How does the protein accomplish these tasks? One expects that the evolutionary pressure exerted by these two requirements has resulted in specific structural features, e.g., highly conserved residues among the various species that are crucial for the function.

In the active site of hemoglobin and myoglobin, the heme iron is coordinated to the four pyrrole nitrogens of the heme and to the N^{ϵ} nitrogen of the proximal histidine, His-F8. Ligands bind to the sixth coordination site of the heme iron from a cavity within the protein, the heme pocket. It contains a highly conserved residue, the distal histidine, His-E7. Textbooks state that this residue plays a functionally important role by stabilizing bound O_2 through a hydrogen bond and rejecting CO by forcing it away from its preferred binding geometry perpendicular to the heme plane (Stryer, 1988). We will show in this communication that steric hindrance is only a minor factor, because the CO binds in a tilted geometry even in the absence of the His-E7 imidazole side chain. Studies of site-specific mutants of His-E7 and other residues, in particular Val-E11, in the distal pocket have helped in clarifying the role of the conserved residues (Braunstein et al., 1988; Olson et al., 1988; Springer et al., 1989; Carver et al., 1990; Balasubramanian et al., 1993).

Fourier-transform infrared (FTIR) spectroscopy is a powerful tool for studying the details of CO binding to heme proteins because of the strong transition dipole of the CO in the infrared. Native sperm whale CO-myoglobin displays three different stretch bands of the CO bound to the heme iron in the region between 1900 and 2000 cm^{-1}. The three stretch

Received for publication 21 May 1993 and in final form 19 August 1993.

Address reprint requests to Dr. G. U. Nienhaus, Department of Physics, University of Illinois at Urbana-Champaign, 1110 West Green Street, Urbana, IL 61801–3080.

D. P. Braunstein's present address is Department of Biochemistry, B476 Beckman Center, Stanford University, Stanford, CA 94305.

H. Frauenfelder's permanent address is MS M715, P-6, Los Alamos National Laboratory, Los Alamos, NM 87545.

J. R. Mourant's present address is MS E535, CLS-5, Los Alamos National Laboratory, Los Alamos, NM 87545.

P. Ormos's permanent address is Biophysics Institute, Hungarian Academy of Sciences, 6701 Szeged, Hungary.

B. A. Springer's present address is DuPont Merck Pharmaceuticals, Biotechnologies/Structural Biology, Wilmington, DE 19880.

R. D. Young's permanent address is Department of Physics, Illinois State University, Normal, IL 61761.

[1] We have already published several papers on ligand binding to heme proteins. Much of the background for the present work has been given in earlier papers (Steinbach et al., 1991; Mourant et al., 1993), in particular paper II in this series (Mourant et al., 1993).

0006-3495/93/12/2447/08 $2.00

bands are assigned to three different conformational substates, denoted as A_0 (1966 cm^{-1}), A_1 (1945 cm^{-1}), and A_3 (1933 cm^{-1}) (Frauenfelder et al., 1991). The *A* substates have the same overall structure, but details differ, e.g., the angle between the heme normal and the CO molecular axis (Ormos et al., 1988; Moore et al., 1988). The population ratios depend strongly on external factors like pH, pressure, and chemical environment (Makinen et al., 1979; Shimada and Caughey, 1982; Brown et al., 1983; Ansari et al., 1987; Hong et al., 1990; Young et al., 1991). The *A* substates, also called taxonomic substates, represent the highest tier in the hierarchical substate model (Ansari et al., 1987; Frauenfelder et al., 1991; Steinbach et al., 1991; Mourant et al., 1993). The rebinding of CO monitored in the *A* bands at cryogenic temperatures is nonexponential, indicating that each of the *A* substates comprises a large number of substates in lower tiers (Ansari et al., 1985; Ansari et al., 1987; Young et al., 1991; Mourant et al., 1993). After photodissociation at cryogenic temperatures, the ligand resides in the distal pocket and absorbs in a number of bands in the region between 2100 and 2200 cm^{-1}, the *B* substates. In a recent paper, we established the connections among the various *A* and *B* substates in sperm whale myoglobin (Mourant et al., 1993).

Although the spectroscopic features of the *A* and *B* substates are well characterized, only a few structural properties of the individual *A* and *B* substates are known so far. In the crystal structure of MbCO at pH 6, the imidazole side chain of the distal histidine resides in the heme pocket (Kuriyan et al., 1986). Phillips and collaborators have recently solved the crystal structure of MbCO at low pH, where almost the entire population is contained in A_0 (Quillin et al., 1992). They find that the imidazole side chain swings out of the heme pocket into the polar solvent environment as it becomes protonated at low pH. Oldfield et al. (1991) performed ab initio calculations of the electrostatic interactions between the His-E7 side chain and an unbound CO molecule restricted to its particular position by the protein. They obtained four different *A* substates arising from two ring-flip isomers in combination with two tautomers ($H^{\delta 1}/H^{\epsilon 2}$). Although this model does not explain the x-ray results regarding the A_0 substate (Quillin et al., 1992), it may still offer a reasonable explanation for the A_1 and A_3 substates. Maxwell and Caughey (1976) originally proposed an A_3 structure consistent with Oldfield's model to account for the low 1933 cm^{-1} frequency of this substate. Transitions between the CS0 are only observed at temperatures above $\approx$160 K, which implies that major conformational rearrangements are involved (Ansari et al., 1987; Young et al., 1991). By contrast, *B* substate transitions occur even at the lowest temperatures measured (T = 4.2 K), which we interpret as motions of the CO ligand in the pocket (Mourant et al., 1993). For the *B* substates, Straub and Karplus (1991) recently performed ab initio calculations in connection with molecular dynamics simulations. They point out that the pronounced red shifts of the *B* bands from the free-gas value of 2143 cm^{-1} cannot be explained by interactions with the distal histidine and speculate that these band positions may arise from binding of the CO to phenylalanine side chains in the pocket.

Studies of infrared spectra of site-specific mutants enable us to assess the influence of particular residues on the *A* and *B* substate spectra. In an earlier paper, we reported that the mutant His(E7)Gly shows an FTIR difference spectrum markedly different from that of native MbCO (Braunstein et al., 1988). Here we extend our study to a number of site-specific mutants at the E7 and/or E11 positions. Besides measuring the spectra, we also determine the orientation of the bound CO with respect to the heme normal by observing the linear dichroism in the infrared after selective photolysis with linearly polarized light at 540 nm.

MATERIALS AND METHODS

Sample preparation

Production of site-directed mutants was performed according to the procedure of Springer and Sligar (1987). The synthetic proteins have an additional Met residue at the amino terminus and the substitution Asn-122 → Asp, but Rohlfs et al. (1990) have shown that kinetic and equilibrium properties are not affected by this modification. Although crystals of this form grow in a different space group than native myoglobin (P6 instead of $P2_1$), the x-ray structure shows only minor structural changes (Phillips et al., 1990). Lyophilized protein was dissolved in 0.1 M glycerol/potassium phosphate buffer (3:1, v/v) to obtain protein solutions at pH 7. A His(E7)Met sample at pH 5.2 was prepared with 0.3 M citrate buffer. The final protein concentrations were in the range 3–6 mM. A microperoxidase (MP-8) sample (Sigma Chemical Co., St. Louis, MO) was prepared similar to the pH 7 protein samples, except that it was loaded under a N_2 atmosphere to prevent rapid oxidation. The proton concentrations were checked with a pH microelectrode (Microelectrodes, Londonderry, NH). Approximately 10 μl of the solution were kept between CaF_2 windows separated by a 75-μm-thick, doughnut-shaped mylar spacer in a sample cell made of oxygen-free, high-conductivity copper.

Low temperature FTIR spectroscopy

The sample cell was attached to the cold-finger of a closed-cycle helium refrigerator (model 22C, CTI Cryogenics, Waltham, MA). The temperature was measured with a silicon diode temperature sensor and adjusted to within 0.1 K by a digital temperature controller (model DRC 93C, Lake Shore Cryotronics Inc., Westerville, OH). The cryogenic set-up was mounted on a FTIR spectrometer (model Sirius 100, Mattson, Madison, WI). Photolysis was achieved by a few seconds of illumination with an Ar ion laser (model 265, Spectra Physics, Mountain View, CA). Transmission spectra were taken before and after illumination in the frequency range between 1800 and 2200 cm^{-1} with a resolution of 2 cm^{-1}. The samples were kept at a temperature of 15 K to ensure that ligand rebinding to all mutants was slow on the experimental time scale. The microperoxidase sample was measured differently: geminate recombination is extremely fast even at 15 K; therefore, the photoproduct spectrum had to be taken under continuous illumination with 300 mW. Absorbance difference spectra were calculated as $\Delta\mathcal{A}(\nu) = -\log[\mathcal{T}_l(\nu)/\mathcal{T}_d(\nu)]$, where $\mathcal{T}_l(\nu)$ and $\mathcal{T}_d(\nu)$ denote the transmittance spectra taken with and without illumination, respectively. To obtain peak positions, linear baseline corrections were applied, and the corrected spectra were fitted with Voigtian line shapes (convolutions of Gaussians and Lorentzians).

Photoselection and linear dichroism

Photoselection and linear dichroism experiments were performed at 15 K. To measure the linear dichroism in the infrared, an IR polarizer (model

IGP228, Molectron, Sunnyvale, CA) was inserted into the IR beam in front of the sample. The sample was illuminated with light from a 250 watt tungsten lamp that passed through a heat filter, a 540-nm interference filter, and a polarizer. The CO was flashed off in small steps with the linearly polarized light. We limited ourselves to maximal photolysis of ≈30% to stay in the linear regime, where the number of photolyzed molecules is proportional to the number of incident photons. Before and after each step, IR transmittance spectra were taken with the IR beam polarized parallel and perpendicular to the polarization of the photolysis beam. The absorption difference spectra were calculated with respect to the spectrum of the unphotolyzed sample for both polarization directions. If we assume that the transition dipole for the electronic absorption lies isotropically in the heme plane and that the IR transition dipole is parallel to the molecular axis of CO, then the angle between the heme normal and the direction of the IR transition dipole of the CO equals (Ormos et al., 1988)

$$\alpha = \arcsin\sqrt{10(r + 0.2)/3}$$

where the anisotropy r equals $(\Delta\mathscr{A}^{\parallel} - \Delta\mathscr{A}_{\perp})/(\Delta\mathscr{A}^{\parallel} + 2\Delta\mathscr{A}_{\perp})$. $\Delta\mathscr{A}^{\parallel}$ and $\Delta\mathscr{A}_{\perp}$ denote the integrated absorbances measured with IR polarization parallel and perpendicular to the polarization of the photolysis beam.

RESULTS AND DISCUSSION

The infrared spectra of the native protein and the His-E7 mutants are shown in Fig. 1, and those of the E11 mutants and microperoxidase in Fig. 2. The positions of the various *A* and *B* substates and the CO angles α are summarized in Table 1.

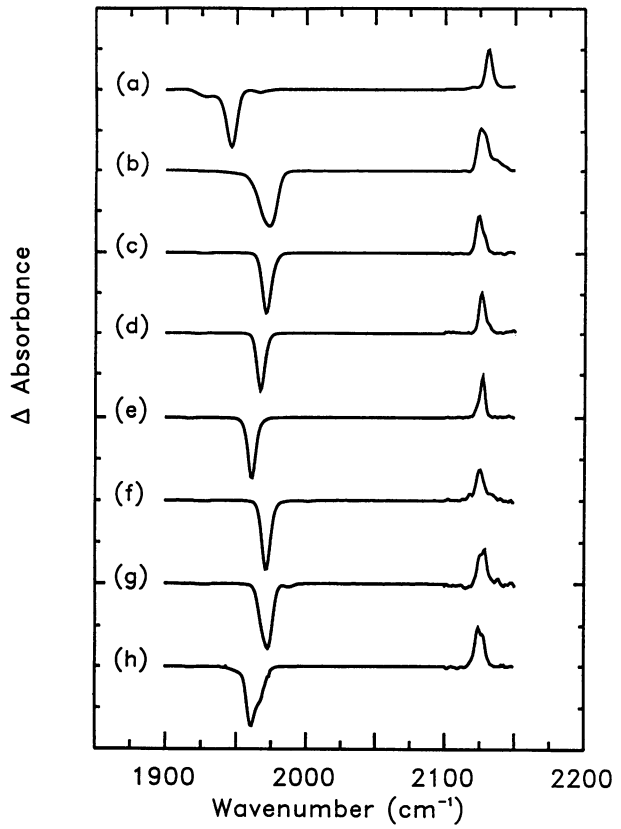

FIGURE 1 FTIR difference spectra of wild-type sperm whale MbCO and mutants at position E7 in glycerol/buffer solutions at pH 7. The IR absorption by the bound CO is shown as negative bands, whereas the IR absorption by the photolyzed CO is shown as positive bands. The absorbances were normalized to equal peak heights. (*a*) wild-type MbCO; (*b*) Mb(E7)GlyCO; (*c*) Mb(E7)ValCO; (*d*) Mb(E7)PheCO; (*e*) Mb(E7)ArgCO; (*f*) Mb(E7)-AspCO; (*g*) Mb(E7)TyrCO; (*h*) Mb(E7)MetCO. Above 2100 cm^{-1}, the ordinate scale is expanded by a factor of 10.

A substate spectra

The spectra of the E7 mutants show either one or two *A* substate lines. The glycine and methionine mutants exhibit two lines very close to each other and difficult to resolve. Only the tyrosine mutant possesses two well separated *A* substates; the one at 1988 cm^{-1} has a rather low occupancy. The observation of multiple *A* substates in the E7 mutants implies that the distal histidine is not essential for the generation of taxonomic substates. However, the strong electrostatic interaction between the imidazole side chain of the distal histidine and the bound CO ligand is clearly the cause for the large separation of the *A* bands in the wild type. In the E7 mutants, the dominant populations tend to cluster near 1966 cm^{-1}, which is the position of the A_0 substate in the native molecule. The A_0 substate is characterized by a charged His-E7 side chain that extends into the solvent, leaving behind an unpolar pocket environment. With the imidazole side chain removed from the CO ligand, its stretch frequency is near 1966 cm^{-1}. Steric factors appear to have only minor effects, and even a bulky residue like phenylalanine does not affect the stretch frequency significantly.

Although His-E7 is highly conserved in hemoglobins and myoglobins, a His-E7 → Gln substitution is found in elephant Mb and in the α-chains of opossum Hb (Romero-Herrera et al., 1981). The main *A* substate appears at 1937 cm^{-1} in elephant Mb (Kerr et al., 1985), which is even lower than the frequency of A_1, the dominant substate of sperm whale myoglobin under physiological conditions. It has been argued that the glutamine side chain is arranged such that its amide group interacts with the bound CO in a similar way as the N^{ϵ} of His-E7 (Park et al., 1991). The His-E7 → Arg

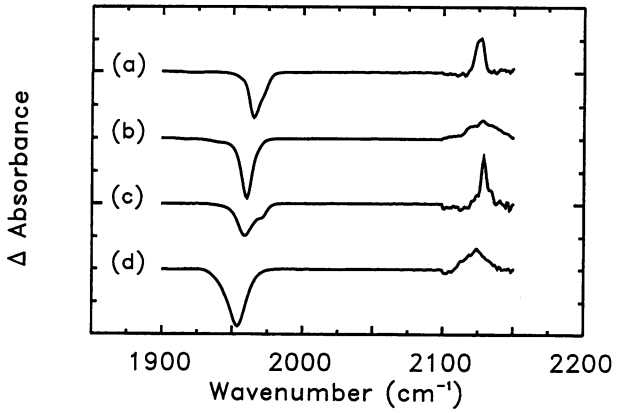

FIGURE 2 FTIR difference spectra of MbCO mutants at position E11 and microperoxidase (MP-8) in glycerol/buffer solutions at pH 7. The stretch bands of the bound and photolyzed CO are shown as negative and positive features, respectively. The absorbances were normalized to equal peak heights. (*a*) Mb(E11)AlaCO; (*b*) Mb(E11)IleCO; (*c*) Mb(E7)Gly(E11)-AlaCO; (*d*) MP-8-CO. Above 2100 cm^{-1}, the ordinate scale is expanded by a factor of 10.

TABLE 1 Band positions (ν) and widths (Γ) of the *A* and *B* substates and angle α between the molecular axis of the bound CO and the heme normal for mutants at the E7 and E11 positions in sperm whale MbCO and for microperoxidase (MP-8-CO).

Species	ν_A (cm^{-1})	Γ_A (cm^{-1})	α(°)	ν_B (cm^{-1})	Γ_B (cm^{-1})
MbCO	1966.4	10.0	15 ± 10	2145.5	12.0
	1945.7	8.3	28 ± 3	2130.6	6.6
	1931.9	19.5	33 ± 4	2118.8	4.0
Mb(E7)GlyCO	1975.1	8.3	20 ± 2	2136.2	11.3
	1968.3	14.1	–	2128.7	6.2
				2124.5	5.5
Mb(E7)ValCO	1971.3	8.4	26 ± 3	2128.1	4.3
				2123.6	5.1
Mb(E7)PheCO	1967.3	7.2	21 ± 2	2131.0	3.8
				2126.0	4.7
Mb(E7)ArgCO	1960.7	7.4	20 ± 2	2127.9	4.0
				2123.5	4.9
Mb(E7)AspCO	1971.3	7.9	20 ± 2	2133.7	10.1
				2124.9	7.6
Mb(E7)TyrCO	1988.2	6.0	–	2129.9	14.8
	1972.9	9.6	23 ± 2	2125.3	6.2
Mb(E7)MetCO	1966.6	9.4	35 ± 1	2131.3	33.1
	1960.3	7.7	24 ± 3	2125.2	7.9
Mb(E11)AlaCO	1970.7	8.7	38 ± 8	2147.2	7.0
	1964.6	9.7	20 ± 2	2125.6	37.1
Mb(E11)IleCO	1960.0	11.2	27 ± 4	2136.3	17.6
	1944.4	25.5	34 ± 5	2127.9	9.2
				2119.5	10.5
Mb(E7)Gly(E11)Ala	1969.8	9.4	–	2129.1	6.1
	1958.7	14.8	–		
MP-8-CO	1953.3	17.9	–	2122.7	17.6

The measurements were done at 15 K. Tilt angles α of the molecular axis of the heme-bound CO with respect to the heme normal were determined by infrared linear dichroism measurements after photoselection with linearly polarized light at 540 nm. Error estimates for the *A* substate positions and widths are ±0.5 cm^{-1}, except for Mb(E11)IleCO and microperoxidase-CO (MP-8-CO), where they are ±1.0 cm^{-1}. Error estimates for the *B* substate positions and widths are ±1.0 cm^{-1}, except for Mb(E11)IleCO and MP-8-CO, where they are ±2.0 cm^{-1}.

mutant has an *A* substate frequency of ≈1961 cm^{-1}, which is low compared with the other E7 mutants (Table 1). In analogy to the glutamine replacement, one might suspect that arginine is also able to position an amide group close to the bound ligand so that the peak frequency gets lowered. In human mutant hemoglobin Zürich, a substitution His-E7 → Arg occurs in the β-subunit, which results in multiple *A* substates at 1951, 1958, and 1968 cm^{-1} (Choc and Caughey, 1981). An x-ray structure of this mutant exists (Tucker et al., 1978), but has not been refined in terms of multiple occupancies of the arginine side chain, so that the structures of the different *A* substates of this mutant remain unknown. The crystal structure shows the arginine side chain salt-bridged to a heme propionate, leaving the pocket wide open. As a consequence, the β-heme subunits autoxidize rapidly. By comparison with other distal pocket mutants, we speculate that the *A* substate at 1968 cm^{-1} arises from a structure where the arginine side chain is removed from the distal pocket. In the 1951 cm^{-1} form, we expect a similar structure as in the elephant myoglobin, with an amide group in close proximity to the CO ligand.

The mutants at position E11 also show interesting features. In the native structure, the Val-E11 side chain imposes steric constraints on the bound CO ligand. In the Val(E11)Ala mutant, the E11 side chain is smaller, and two *A* substates are found closely together at 1965 and 1971 cm^{-1}. The *A* substate frequencies are similar to the A_0 substate position in native myoglobin, but there is no reason to assume that the imidazole side chain of His-E7 is removed from the pocket in this mutant at pH 7. Most likely, the CO orients itself differently with respect to the His-E7 side chain, with concomitant differences in the electrostatic interaction. The Val(E11)Ile mutant has the lowest CO affinity of all E7 or E11 mutants studied so far. It has been suggested that the methyl group on the β-carbon is close to the heme iron and interferes with the final binding step (Balasubramanian et al., 1993). The bulkier isoleucine side chain leads to an *A* substate at 1960 cm^{-1} and a second, weakly populated one at 1944 cm^{-1}. Finally, the double mutant His(E7)Gly/Val(E11)Ala, also shows two *A* substates near pH 7.

In native sperm whale MbCO, the relative populations of A_0 and A_1 depend on pH; they are connected to the titration of the distal histidine. For the His(E7)Met mutant, we have studied the pH dependence of its two *A* substates. Fig. 3 shows spectra taken at 100 and 295 K on samples at pH 5.2 and 7.3. The spectra of this mutant at 295 K are distinctly different for the two pH values. At 100 K, we observe a single *A* substate at 1967 cm^{-1} in the pH 5.2 sample, whereas the spectrum at pH 7.3 appears to be a superposition of two bands at 1960 and 1967 cm^{-1}. We conclude that there are two different *A* substates in the His(E7)Met mutant; their populations depend on pH. Further evidence comes from the CO angles which are considerably different for the two states (see Table 1). As the methionine side chain itself does not respond

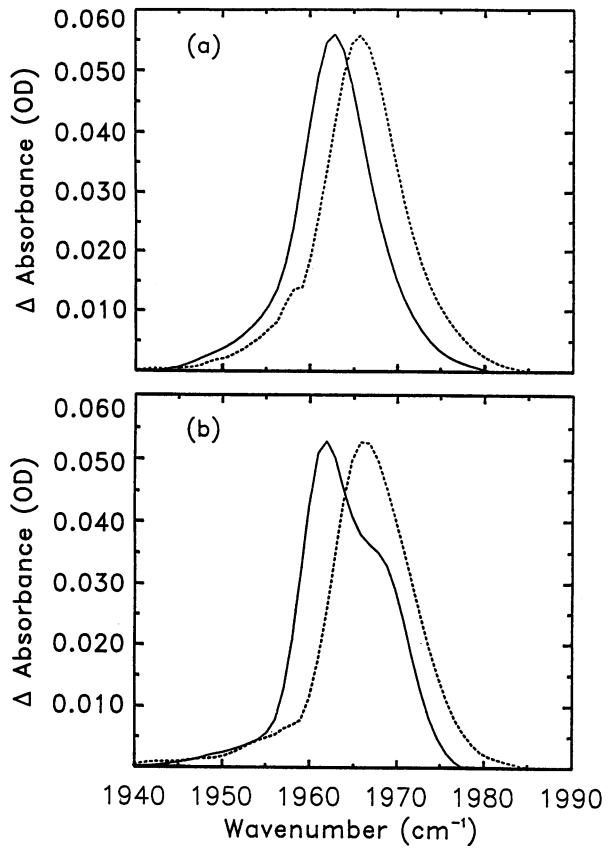

FIGURE 3 FTIR difference spectra of Mb(E7)MetCO at pH 7.3 (*solid line*) and pH 5.2 (*dashed line*). (*a*) T = 295 K; (*b*) T = 100 K.

to pH changes, the pH effect must arise from a pH-dependent structural change, probably due to the titration of a nearby residue with $pK_a \approx 6$. A possible candidate for the observed pH titrations in His(E7)Met is His-FG3, a residue on the proximal side that is in contact with the heme. This residue has a pK_a of 5.7 at room temperature (Krishnamoorti and La Mar, 1984), from which we estimate an apparent pK_a near 7 at cryogenic temperatures,[2] consistent with the spectra shown in Fig. 3. Although the role of distal pocket mutants in ligand binding has been discussed in great detail (Olson et al., 1988; Springer et al., 1989; Morikis et al., 1989; Egeberg et al., 1990), little attention has been paid so far to residues on the proximal side. A number of studies have revealed the existence of a titratable group in the pK_a range 5–6 that affects the oxygen binding affinity (La Mar et al., 1978), the room temperature CO binding kinetics (Doster et al., 1982), the spectrum of the α-band (Fuchsman and Appleby, 1978), and the population of the A substates in bovine myoglobin (Shimada and Caughey, 1982).

For the glycine mutant, a single, broad band at 1973 cm^{-1} was reported previously (Braunstein et al., 1988), but it was then already mentioned that the band is composed of two kinetically distinguishable components. Lowering the pH leads to a shift of the A band to 1968 cm^{-1} (data not shown), similar to the effect observed with the methionine mutant.

Resonance Raman spectroscopy is an experimental method that often complements the results from infrared absorption. Champion and collaborators (Morikis et al., 1989) were the first to study the Raman frequencies and relative intensities of the iron-ligand stretch vibration ν_{FeC} and the CO stretch vibration ν_{CO} in the His(E7)Met and His(E7)Gly mutants. These two stretch frequencies are known to exhibit an inverse correlation (Uno et al., 1987; Li and Spiro, 1988). Therefore, the A_0 substate in native sperm whale myoglobin has the highest CO stretch and the lowest iron-ligand stretch frequency, ν_{FeC} = 491 cm^{-1}; for A_1, ν_{FeC} = 508 cm^{-1}, and for A_3, ν_{FeC} = 518 cm^{-1} (Morikis et al., 1989). For the mutants His(E7)Met and His(E7)Gly, a pH-independent doublet structure was reported for ν_{FeC}, with the two Raman lines at positions similar to those of A_0 and A_1 in the native protein. Furthermore, CO stretch Raman lines were assigned for the A_1 substate, for His(E7)Met, ν_{CO} = 1944 cm^{-1}, and for His(E7)Gly, ν_{CO} = 1947 cm^{-1}. Our FTIR studies do not give a hint for an A_1-like substate in these mutants, and the two A substate lines that we observe are pH-dependent. Thus, the presence of the A_1 state in the resonance Raman analysis of these mutants (Morikis et al., 1989) may need to be reconsidered.

B substate spectra

The B substate spectra of all the mutants cluster between 2120 and 2135 cm^{-1}. In native MbCO, the main B substates are found at 2119 and 2131 cm^{-1} (Mourant et al., 1993). The similarity of the wavenumbers implies that neither His-E7 nor Val-E11 are major determinants affecting the B substate positions. Earlier, we showed that multiple B substates exist for a single A substate (Alben et al., 1982; Mourant et al., 1993). The presence of multiple B substates in the His(E7)-Val mutant, which has only a single A substate, makes this point even stronger. Usually, the B substate lines are significantly narrower than the A bands, indicative of a highly ordered environment and fixed CO positions. In this regard, the B substate spectrum of the Val(E11)Ile mutant in Fig. 2 is particularly interesting: it shows a broad, featureless band, extending from 2100 to 2150 cm^{-1}. The Val(E11)Ile mutant is known for very slow ligand binding. This property is attributed to the presence of the methyl group on the β-carbon of the isoleucine side chain, which interferes with the ligand at the binding site. The leucine mutant, where the methyl group sits on the γ-carbon, does not show this behavior. One may speculate that the isoleucine side chain prevents the ligand from binding to the highly ordered docking site that leads to a sharp B substate line and fast binding. But then the

[2] Acid/base equilibria of protein titratable groups and buffer depend on temperature. Here we use the temperature dependence of the A_0/A_1 substate populations of native sperm whale myoglobin, which reflect the protonation of His-E7, to obtain an estimate for the effect. At room temperature, equal populations are found in samples with pH ≈ 4.4. To obtain equal populations at low temperatures, the sample pH has to be near 5.7 at room temperature. If we assume a similar change for His-FG3, we obtain an apparent $pK_a \approx 7$ at low temperatures for this residue.

B substate docking site of the CO must be close to the heme, maybe even at the heme iron itself.

More support for the close association of the *B* substates to the heme comes from the microperoxidase spectrum. Microperoxidase (MP-8) is a digested horse heart cytochrome with eight amino acids bound to a heme. It possesses a proximal histidine, but no protein residue on the ligand binding side. The *B* state spectrum of MP-8-CO exhibits a broad peak covering the region between 2100 and 2150 cm^{-1} with the maximum at 2124 cm^{-1}. Just as in heme proteins, we observe considerable red shifts of the IR absorption. Because there are no amino acid residues on the distal side, the photodissociated ligand is either in contact with the polar solvent molecules or with the heme; coupling to protein residues cannot account for the observed spectral features. Matrix isolation studies at low temperatures report blue-shifted IR bands of CO in polar solvents between 2148 and 2155 cm^{-1} (Dubost et al., 1972; Diema and Lee, 1982; Gebecki and Krantz, 1984; Tso and Lee, 1985). Therefore, the presence of the glycerol/water matrix cannot explain the red shift in microperoxidase. We conclude that the positions of the *B* bands are influenced by interactions of the photodissociated ligand with the heme, possibly even with the heme iron itself. The broad absorption in microperoxidase and Val(E11)Ile most likely arises from the strong disorder of the environment in the proximity of the photodissociated ligand.

The results obtained here, together with earlier work, suggest the following scenario for the ligand binding reaction at low temperatures. On photodissociation, the CO leaves the binding site at the heme iron with considerable kinetic energy, collides a few times with pocket residues, and finally comes to rest at a site where it is weakly bound. Experimental evidence and computer simulations indicate that the *B* states are formed within a few hundred femtoseconds (Anfinrud et al., 1988; Petrich et al., 1991). The present data imply that this binding site is close to the heme iron. This view is supported by rebinding experiments below 10 K, where tunneling barriers of 0.5–1 Å were obtained (Alberding et al., 1976; Frauenfelder, 1979). Further support comes from EXAFS experiments: Chance et al. (1983) and Powers et al. (1987) reported that the CO was still in the first coordination shell after photodissociation at low temperatures and only displaced by 0.05 Å from the heme iron. This result was criticized as being inconsistent with optical, infrared, and magnetic susceptibility studies (Fiamingo and Alben, 1985). Another EXAFS investigation confirmed that the CO was still in the first shell, but gave a displacement of 0.27–0.45 Å (Teng et al., 1987). Eisenstein et al. (1978) performed iterative extended Hückel self-consistent charge calculations of model systems and obtained weak binding to the high-spin iron. Taken together, these investigations provide strong evidence for the closeness of the photodissociated CO to the heme iron.

CO orientation

The angle α between the CO molecular axis and the heme normal can arise from three different ways in which the heme–CO geometry can be distorted, (i) tilting, where the Fe–C–O unit is linear and oriented away from the heme normal, (ii) bending, where the Fe–C bond is normal to the heme plane, and only the oxygen is displaced, and (iii) buckling of the heme. Effects of these distortions on vibrational bands have been discussed in detail by Li and Spiro (1988). Linear dichroism experiments measure the angle between the CO axis and the heme normal. Therefore, the data summarized in Table 1 may be combinations of the three distortions mentioned above. The angles are between 20° and 38° for the various E7 mutants. In the case of His(E7)Val, where one expects no steric hindrance of the CO by the valine residue, the angle α is similar to that of the dominant A_1 substate of the native structure. The angle α therefore appears rather insensitive to the size of the residue at the E7 position. There seems to be enough space in the pocket to accommodate both the ligand and a bulky side chain at the position E7 without major steric hindrance. These observations contradict the traditional textbook knowledge that His-E7 forces the CO into an off-axis position (Stryer, 1988). The E11 mutants show even larger angles than the ones found in the native structure, implying that the E11 residue may affect the orientation of the CO more than the E7 residue.

Conclusions

Comparison of the various distal pocket mutants of sperm whale myoglobin points to the intimate connection of the taxonomic substates A_0, A_1, and A_3 of the native structure to the presence of His-E7. Without appreciable interaction with a distal pocket residue, the bound CO absorbs near 1966 cm^{-1}, the position of A_0. On substitution of His-E7 with an unpolar side chain, we still find more than one *A* substate, although with smaller separation, indicating a weaker coupling of the bound CO to other titratable groups. The CO binds in an off-axis position to all E7 mutants, with the angle $\alpha \geq 20°$. Thus, the His-E7 side chain does *not* force the CO into an off-axis position. Its physiological importance most likely rests on its ability to stabilize O_2 ligands with a hydrogen bond to its N^{ϵ} proton. Furthermore, it has been suggested by Perutz that an important function of His-E7 is the removal of protons from the distal pocket to prevent autoxidation (Perutz, 1989). Finally, because the three *A* substates bind CO (and presumably also O_2) with different rates, the dependence of their populations on external parameters may permit control of binding.

The *B* substate spectra of the different mutants are similar to that of the native structure, but details differ. The *B* substate spectra of the His(E7)Ile mutant and of microperoxidase lead us to the conclusion that the photodissociated ligand stays close to the heme iron after photolysis.

We thank Y. Abadan, B. T. Banko, D. Ehrenstein, C. Eng, R. Ernst, M. Filiaci, D. C. Lamb, B. McMahon, J. Müller, and R. Philipp for their collaboration.

This work was supported by the National Science Foundation (Grant DMB87–16476) and the National Institutes of Health (Grants GM 18051, 31656 and 33775).

REFERENCES

Alben, J. O., D. Beece, S. F. Bowne, W. Doster, L. Eisenstein, H. Frauenfelder, D. Good, J. D. McDonald, M. C. Marden, P. P. Moh, L. Reinisch, A. H. Reynolds, E. Shyamsunder, and K. T. Yue. 1982. Infrared spectroscopy of photodissociated carboxymyoglobin at low temperatures. *Proc. Natl. Acad. Sci. USA.* 78:2903–2907.

Alberding, N., R. H. Austin, K. W. Beeson, S. S. Chan, L. Eisenstein, H. Frauenfelder, and T. M. Nordlund. 1976. Tunneling in ligand binding to heme proteins. *Science.* 192:1002–1004.

Anfinrud, P. A., C. Han, and R. M. Hochstrasser. 1989. Direct observations of ligand dynamics in hemoglobin by subpicosecond infrared spectroscopy. *Proc. Natl. Acad. Sci. USA.* 86:8387–8391.

Ansari, A., J. Berendzen, D. Braunstein, B. R. Cowen, H. Frauenfelder, M. K. Hong, I. E. T. Iben, J. B. Johnson, P. Ormos, T. B. Sauke, R. Scholl, A. Schulte, P. J. Steinbach, J. Vittitow, and R. D. Young. 1987. Rebinding and relaxation in the myoglobin pocket. *Biophys. Chem.* 26:337–355.

Ansari, A., J. Berendzen, S. F. Bowne, H. Frauenfelder, I. E. T. Iben, T. B. Sauke, E. Shyamsunder, and R. D. Young. 1985. Protein states and proteinquakes. *Proc. Natl. Acad. Sci. USA.* 82:5000–5004.

Balasubramanian, S., D. G. Lambright, M. C. Marden, and S. G. Boxer. 1993. CO recombination to human myoglobin mutants in glycerol-water solutions. *Biochemistry.* 32:2202–2212.

Braunstein, D., A. Ansari, J. Berendzen, B. R. Cowen, K. D. Egeberg, H. Frauenfelder, M. K. Hong, P. Ormos, T. B. Sauke, R. Scholl, A. Schulte, S. G. Sligar, B. A. Springer, P. J. Steinbach, and R. D. Young. 1988. Ligand binding to synthetic mutant myoglobin (His-E7 → Gly): role of distal histidine. *Proc. Natl. Acad. Sci. USA.* 85:8497–8501.

Brown, W. E., J. W. Sutcliffe, and P. D. Pulsinelli. 1983. Multiple internal reflectance infrared spectra of variably hydrated hemoglobin and myoglobin films: effects of globin hydration on ligand conformer dynamics and reactivity at the heme. *Biochemistry.* 22:2914–2923.

Carver, T. E., R. J. Rohlfs, J. S. Olson, Q. H. Gibson, R. S. Blackmore, B. A. Springer, and S. G. Sligar. 1990. Analysis of the kinetic barriers for ligand binding to sperm whale myoglobin using site-directed mutagenesis and laser photolysis techniques. *J. Biol. Chem.* 265:20007–20020.

Chance, B., R. Fischetti, R., and L. Powers. 1983. Structure and kinetics of the photoproduct of carboxymyoglobin at low temperatures: an x-ray absorption study. *Biochemistry.* 22:3820–3829.

Choc, M. G., and W. S. Caughey. 1981. Evidence from infrared and ^{13}C NMR spectra for discrete rapidly interconverting conformers at the carbon monoxide binding sites of hemoglobins A and Zürich. *J. Biol. Chem.* 256:1831–1838.

Collman, J. P., J. I. Brauman, T. R. Halbert, and K. S. Suslick. 1976. Nature of O_2 and CO binding to metalloporphyrins and heme proteins. *Proc. Natl. Acad. Sci. USA.* 73:3333–3337.

Diem, M., and E. K. C. Lee. 1982. Photooxidation of formaldehyde in solid oxygen and argon/oxygen matrices at 12 K. *J. Phys. Chem.* 86: 4507–4512.

Doster, W., D. Beece, S. F. Bowne, E. E. Di Iorio, L. Eisenstein, H. Frauenfelder, L. Reinisch, E. Shyamsunder, K. H. Winterhalter, and K. T. Yue. 1982. Control and pH dependence of ligand binding to heme proteins. *Biochemistry.* 21:4831–4839.

Dubost, H., and L. Abouaf-Marguin. 1972. Infrared spectra of carbon monoxide trapped in solid argon. Double-doping experiments with H_2O, NH_3 and N_2. *Chem. Phys. Lett.* 17:269–273.

Egeberg, K. D., B. A. Springer, S. G. Sligar, T. E. Carver, R. J. Rohlfs, and J. S. Olson. 1990. The role of Val^{68}(E11) in ligand binding to sperm whale myoglobin. *J. Biol. Chem.* 265:11788–11795.

Eisenstein, L., D. R. Franceschetti, and K. L. Yip. 1978. Iterative extended Hückel studies of some pyridine-Fe(II)-porphin complexes. *Theor. Chim. Acta.* 49:349–359.

Fiamingo, F. G., and J. O. Alben. 1985. Structures of photolyzed carboxymyoglobin. *Biochemistry.* 24:7964–7970.

Frauenfelder, H. 1979. Molecular tunneling in heme proteins. *In* Tunneling in Biological Systems. Academic Press, Inc., New York. 627–649.

Frauenfelder, H., S. G. Sligar, and P. G. Wolynes. 1991. The energy landscapes and motions of proteins. *Science.* 254:1598–1603.

Fuchsman, W. H., and C. A. Appleby. 1979. CO and O_2 complexes of soybean leghemoglobins: pH effects upon infrared and visible spectra. Comparisons with CO and O_2 complexes of myoglobin and hemoglobin. *Biochemistry.* 18:1309–1321.

Gebecki, J., and A. Krantz. 1984. Substituent effects on weakly bound complexes of phenols and carbon monoxide in argon matrices, hydrogen bonding at cryogenic temperatures. *J. Am. Chem. Soc.* 106:8097–8104.

Hong, M. K., D. Braunstein, B. R. Cowen, H. Frauenfelder, I. E. T. Iben, J. R. Mourant, P. Ormos, R. Scholl, A. Schulte, P. J. Steinbach, A. Xie, and R. D. Young. 1990. Conformational substates and motions in myoglobin: external influences on structure and dynamics. *Biophys. J.* 58: 429–436.

Kerr, E. A., N. Yu, D. Bartnicki, and H. Mizukami. 1985. Resonance Raman studies of CO and O_2 binding to elephant myoglobin (distal His(E7) → Gln). *J. Biol. Chem.* 260:8360–8365.

Krishnamoorthi, R., and G. N. La Mar. 1984. Identification of the titrating group in the heme cavity of myoglobin. Evidence for the heme-protein π–π interaction. *Eur. J. Biochem.* 138:135–140.

Kuriyan, J., S. Wilz, M. Karplus, and G. A. Petsko. 1986. X-ray structure and refinement of carbon-monoxy (FeII)-myoglobin at 1:5 Å resolution. *J. Mol. Biol.* 192:133–154.

La Mar, G. N., D. L. Budd, D. B. Viscio, K. M. Smith, and K. C. Langry. 1978. Proton nuclear magnetic resonance characterization of heme disorder in hemoproteins. *Proc. Natl. Acad. Sci. USA.* 75:5755–5759.

Li, X. Y., and T. G. Spiro. 1988. Is bound CO linear or bent in heme proteins? Evidence from resonance Raman and infrared spectroscopic data. *J. Am. Chem. Soc.* 110:6024–6033.

Makinen, M. W., R. A. Houtchens, and W. S. Caughey. 1979. Structure of carboxymyoglobin in crystals and in solution. *Proc. Natl. Acad. Sci. USA.* 76:6042–6046.

Maxwell, J. C., and W. S. Caughey. 1976. An infrared study of NO bonding to heme B and hemoglobin A. Evidence for inositol hexaphosphate induced clevage of proximal histidine to iron bonds. *Biochemistry.* 15: 388–396.

Moore, J. N., P. A. Hansen, and R. M. Hochstrasser. 1988. Iron-carbonyl bond geometries of carboxymyoglobin and carboxyhemoglobin in solution determined by picosecond time-resolved infrared spectroscopy. *Proc. Natl. Acad. Sci. USA.* 85:5062–5066.

Morikis, D., P. M. Champion, B. A. Springer, and S. G. Sligar. 1989. Resonance Raman investigations of site-directed mutants of myoglobin: effects of distal histidine replacement. *Biochemistry.* 28:4791–4800.

Mourant, J. R., D. P. Braunstein, K. Chu, F. Frauenfelder, G. U. Nienhaus, P. Ormos, and R. D. Young. 1993. Ligand binding to heme proteins: II. Transitions in the heme pocket of myoglobin. *Biophys. J.* 65:1496–1507.

Oldfield, E., K. Guo, J. D. Augspurger, and C. E. Dykstra. 1991. A molecular model for major conformational substates in heme proteins. *J. Am. Chem. Soc.* 113:7537–7541.

Olson, J. S., A. J. Mathews, R. J. Rohlfs, B. A. Springer, K. D. Egeberg, S. G. Sligar, J. Tame, J. P. Renaud, and K. Nagai. 1988. The role of the distal histidine in myoglobin and haemoglobin. *Nature.* 336:265–266.

Ormos, P., D. Braunstein, H. Frauenfelder, M. K. Hong, S. L. Lin, T. B. Sauke, and R. D. Young. 1988. Orientation of carbon monoxide and structure-function relationship in carbonmonoxymyoglobin. *Proc. Natl. Acad. Sci. USA.* 85:8492–8496.

Park, K. D., K. Guo, F. Adebodun, M. L. Chiu, S. G. Sligar, and E. Oldfield. 1991. Distal and proximal ligand interactions in heme proteins: Correlations between C-O and Fe-C vibration frequencies, oxygen-17 and carbon-13 nuclear magnetic resonance chemical shifts, and oxygen-17 nuclear quadrupole coupling constants in $C^{17}O$- and ^{13}CO-labeled species. *Biochemistry.* 30:2333–2347.

Perutz, M. F. 1989. Myoglobin and haemoglobin: role of distal residues in reactions with haem ligands. *Trends Biochem. Sci.* 14:42–44.

Phillips, G. N. Jr., R. M. Arduini, B. A. Springer, and S. G. Sligar. 1990. Crystal structure of myoglobin form a synthetic gene. *Proteins Struct. Funct. Genet.* 7:358–365.

Petrich, J. W., J.-C. Lambry, K. Kuczera, M. Karplus, C. Poyart, and J.-L. Martin. 1991. Ligand binding and protein relaxation in heme proteins: a room temperature analysis of NO geminate recombination. *Biochemistry.* 30:3975–3987.

Powers, L., B. Chance, M. Chance, B. Campbell, J. Friedman, S. Khalid, C. Kumar, A. Nagui, K. S. Reddy, and Y. Zhou. 1987. Kinetic, structural, and spectroscopic identification of geminate states of myoglobin: a ligand binding site on the reaction pathway. *Biochemistry.* 26:4785–4796.

Quillin, M. L., R. E. Brantley Jr., K. A. Johnson, and G. Phillips. 1992. Kinetic and structural analysis of the effects of pH on carbon monoxide association in myoglobin. *Biophys. J.* 61:A466.

Rohlfs, R. J., A. J. Mathews, T. E. Carver, J. S. Olson, B. A. Springer, K. D. Egeberg, and S. G. Sligar. 1990. The effects of amino acid substitution

at position E7 (residue 64) on the kinetics of ligand binding to sperm whale myoglobin. *J. Biol. Chem.* 265:3168–3176.

Romero-Herrera, A. E., M. Goodman, H. Dene, D. E. Bartnicki, and H. Mizukami. 1981. An exceptional amino acid replacement on the distal side of the iron atom in proboscidean myoglobin. *J. Mol. Evol.* 17: 140–147.

Shimada, H., and W. S. Caughey. 1982. Dynamic protein structures: effects of pH on conformer stabilities at the ligand-binding site of bovine heart myoglobin carbonyl. *J. Biol. Chem.* 257:11893–11900.

Springer, B. A., and S. G. Sligar. 1987. High-level expression of sperm whale myoglobin in *Escherichia coli*. *Proc. Natl. Acad. Sci. USA.* 84: 8961–8965.

Springer, B. A., K. D. Egeberg, S. G. Sligar, R. J. Rohlfs, A. J. Mathews, and J. S. Olson. 1989. Discrimination between oxygen and carbon monoxide and inhibition of autooxidation by myoglobin. Site-directed mutagenesis of the distal histidine. *J. Biol. Chem.* 264:3057–3060.

Steinbach, P. J., A. Ansari, J. Berendzen, D. Braunstein, K. Chu, B. R. Cowen, D. Ehrenstein, H. Frauenfelder, J. B. Johnson, D. C. Lamb, S. Luck, J. R. Mourant, G. U. Nienhaus, P. Ormos, R. Philipp, A. Xie, and R. D. Young. 1991. Ligand binding to heme proteins: the connection between dynamics and function. *Biochemistry.* 30:3988–4001.

Straub, J. E., and M. Karplus. 1991. Molecular dynamics study of the photodissociation of carbon monoxide from myoglobin: ligand dynamics in the first 10 ps. *Chem. Phys.* 158:221–248.

Stryer, L. 1988. *Biochemistry.* 3rd Ed. Freeman Publications, San Francisco, CA.

Teng, T.-Y., H. W. Huang, and G. A. Olah. 1987. 5 K extended x-ray absorption fine structure and 40 K 10-s resolved extended x-ray absorption fine structure studies of photolyzed carboxymyoglobin. *Biochemistry.* 26:8066–8072.

Tso, T. L., and E. K. C. Lee. 1985. FTIR spectra of the hydrogen bonding in matrix-isolated molecular complexes of hydrogen oxides, carbon monoxide, and carboy dioxide formed in the photooxidation of isotropic formaldehydes and glyoxal in solid O_2 at 12–15 K. *J. Phys. Chem.* 89: 1618–1631.

Tucker, P. W., S. E. V. Phillips, M. F. Perutz, R. Houtchens, and W. S. Caughey. 1978. Structure of hemoglobins Zürich [His E7(63)$\beta \rightarrow$ Arg] and Sydney [Val E11(67)$\beta \rightarrow$ Ala] and role of the distal residues in ligand binding. *Proc. Natl. Acad. Sci. USA.* 75:1076–1080.

Uno, T., Y. Nishimura, M. Tsuboi, R. Makino, T. Iizuka, and Y. Ishimura. 1987. Two types of conformers with distinct Fe-C-O configuration in the ferrous CO complex of horseradish peroxidase. *J. Biol. Chem.* 262: 4549–4556.

Young, R. D., H. Frauenfelder, J. B. Johnson, D. C. Lamb, G. U. Nienhaus, R. Philipp, and R. Scholl. 1991. Time- and temperature dependence of large-scale conformational transitions in myoglobin. *Chem. Phys.* 158: 315–328.